Optical Anisotropy in Single Light-Emitting Polymer Nanofibers

Stefano Pagliara,[†,‖] Miriam S. Vitiello,[‡,¶] Andrea Camposeo,*[,†] Alessandro Polini,[†] Roberto Cingolani,[§] Gaetano Scamarcio,[‡] and Dario Pisignano*[,†,⊥]

[†]National Nanotechnology Laboratory of Istituto Nanoscienze—CNR, and [⊥]Dipartimento di Ingegneria dell'Innovazione, Università del Salento, via Arnesano, I-73100 Lecce, Italy

[‡]CNR—Istituto di Fotonica e Nanotecnologie, UOS Bari and Physics Department, University of Bari "Aldo Moro", via Amendola 173, I-70126 Bari, Italy

[§]Istituto Italiano di Tecnologia (I.I.T.), via Morego 30, I-16163 Genova, Italy

ABSTRACT: We investigate the optical anisotropy of single nanofibers realized by electrospinning a conjugated polymer. Polarized infrared and micro-Raman measurements evidence a higher degree of molecular orientation in fibers processed from tetrahydrofuran solutions, with respect to samples spun from mixture with dimethyl sulfoxide. The fraction of ordered molecules is correlated to the fibers morphology. Polarized photoluminescence highlights a larger red shift (60 meV) for spectra from fibers processed from tetrahydrofuran, confirming

the higher achieved molecular order resulting in reduced interchain separation and hence excitonic emission with lower transition energies compared to that from randomly aligned molecules. Conjugated polymer fibers are obtained, emitting light with polarization ratios up to 5, usable as polarized photonic nanosources.
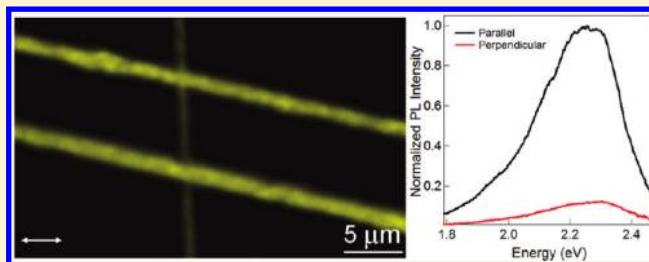
1. INTRODUCTION

Conjugated polymers exhibit advantages such as high mechanical flexibility, low-cost processing, and tailor-made functionalities, together with their general strong intra- and weak intermolecular interactions.[1] Importantly, the resulting optical or electrical anisotropy can be effectively improved by favoring molecular orientation along preferential axes, thus enhancing charge transport[2,3] and optical confinement[4−6] and leading to better performances when applied to photonic, optoelectronic, or lab-on-chip devices.[7,8] Different technologies are proposed to obtain uniaxial molecular alignment within conjugated polymer systems, such as tensile drawing,[9] mechanical stretching or rubbing,[10,11] thermotropic liquid-crystal phase formation,[12] Langmuir−Blodgett deposition,[13] or nanoconfinement during imprinting.[14] All these methods are mainly focused on the deposition and orientation of thin films.

Alternatively, electrospinning (ES) allows the realization of conjugated polymer nanofibers,[15,16] intrinsically promoting the molecular orientation thanks to the elongated and stretched polymer jet formed by the high applied electric field.[17] In particular, fully conjugated polymer nanofibers have been reported only recently,[15] because of the limited solubility and relatively poor viscoelastic behavior of these materials. Exploiting suitable mixtures of ES solvents and nonsolvents may help to process conjugated polymers;[15] however, they affect the achievable fiber morphology and optical anisotropy. In fact, the ES jet exhibits a complex fluid behavior[18,19] strongly related to the solution properties,[20] which consequently impacts on the degree of induced molecular orientation and its uniformity over the length of the fiber. Investigating the alignment at a molecular level and

its correlation with the ES processing conditions is therefore mandatory, aiming to develop devices based on organic nanofibers with enhanced optical anisotropy.

Besides wide-angle X-ray diffraction,[21] polarized infrared[22,23] and Raman spectroscopies[17] are used to study the molecular alignment, avoiding damages to the optical properties. These are powerful structural probes for conjugated polymers, allowing to evaluate both molecular and transition dipole moment orientation, when combined to polarized absorption measurements.[12,24]

Here we investigate for the first time the optical anisotropy of light-emitting nanofibers, by the conjugated polymer, poly[(9,9-dioctylfluorenyl-2,7-diyl)-co-(1,4-benzo-{2,1'-3}-thiadiazole)] (F8BT). For ES we use either tetrahydrofuran (THF) solutions or mixtures of THF and dimethyl sulfoxide (DMSO). Polarized infrared, micro-Raman, and photoluminescence (PL) measurements evidence that THF solutions lead to more ordered molecular chains, without nanoscale aggregates as occurring in fibers spun from the mixture. Overall, PL polarization ratios up to 5 are obtained in F8BT fibers, opening the way for exploiting polyfluorenes in polarized light nanosources for photonic applications.

2. EXPERIMENTAL SECTION

2.1. Electrospinning. The light-emitting conjugated polymer F8BT (molecular weight 141 kg/mol, American Dye Source Inc.) is dissolved in THF (Fluka) and in a 9:1 w-w THF/DMSO

(Sigma Aldrich) mixture (0.8 mM). Using a nonsolvent with high boiling point and dielectric constant favors ES of conjugated polymers.[15] ES is performed by placing about 0.2 mL of solution into a 1.0 mL plastic syringe tipped with a 27-gauge stainless steel needle. The positive lead from a high voltage supply (XRM30P, Gamma High Voltage Research) is connected to the metal needle applying a bias around 5 kV. The solution is injected into the needle at a constant rate of 2 μL/min by a syringe pump (33 Dual Syringe Pump, Harvard Apparatus), which prevents dripping at the end of the metallic capillary. A stripe collector, composed of two 2 mm thick Al regions mutually separated by 1.5–2.0 cm and biased at −2 kV, is placed at a distance of about 8 cm from the needle. Free-standing fibers through the electrodes are finally collected on 1×1 cm^2 Si substrates for optical investigation. The DMSO/THF mixture is generally found to allow a higher throughput of electrospun fibers (enhancement >75% on the ES collector for depositions over 1 min).

Uniaxially aligned arrays of fibers are obtained by using as collector a metallic disk (diameter 8 cm, thickness 1 cm) mounted on a mandrel (RT Collector, Linari Engineering Srl) rotating at 4000 rpm, placed at about 10 cm from the needle and biased at a negative voltage of −6 kV. The collection time is about 60 min.

All the ES experiments are performed at room temperature with air humidity about 40%.

2.2. Characterization. Scanning electron microscopy (SEM) is performed by a Raith 150 electron beam system with an acceleration voltage around 3 kV and an aperture size of 30 μm. A 10 nm thick Au film is deposited on fibers by physical vapor deposition (Kurt J. Lesker) prior investigation.

For polarized optical microscopy (POM), the unpolarized light from the halogen lamp of an upright microscope (BX52, Olympus) is linearly polarized by an absorption polarizer and directed through the microscope objectives to single fibers. The fibers are imaged through the same microscope objective, analyzed by a linear polarizer, and finally analyzed by a Digital Camera (8 Megapixels, DFC 490, Leica).

Polarized Fourier transform infrared (FTIR) spectroscopy is carried out by employing a FTIR spectrophotometer (Spectrum 100, Perkin-Elmer Inc.), equipped with a IR grid polarizer (Specac Limited, U.K.), consisting of 0.12 μm wide strips of aluminum. The 1.6 mm wide beam, incident orthogonally to the plane of the sample, is polarized alternatively parallel or orthogonal to the fibers alignment main axis.

Raman spectra are collected by focusing the 647 nm line of a cw Kr$^+$ laser with intensity 3×10^4 W·cm^{-2} on the fibers, down to a spot of about 1 μm diameter by using an 80× long working distance plano-achromatic microscope objective lens. The Rayleigh scattering of the laser light is blocked by means of a Notch filter. A $\lambda/2$ waveplate is inserted in the beam path prior to the microscope entrance to allow rotation of the polarization of the incident radiation. A polarizer is inserted before the Notch filter to select the appropriate polarization of the analyzed light. For each polarization condition, the Raman spectra are compared with those collected by rotating the fiber by 90°. In this way, the contributions introduced by each polarizer and by the optical microscope are properly accounted for. In all the investigated polarization configurations, a backscattering geometry is used, with a wave vector, $q = 2k_Y = 4\pi n(\lambda)/\lambda = 0.75 \times 10^6$ cm^{-1}, where k_Y, n, and λ indicate the wavenumber, refractive index, and wavelength, respectively. The position of the incident laser spot is varied along the fiber axis by means of a XZ translation stage
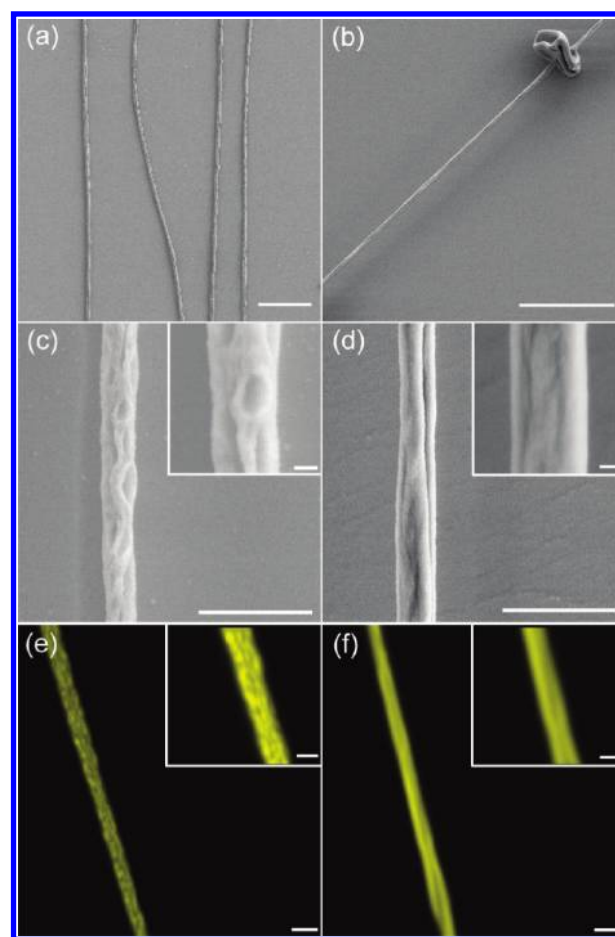

Figure 1. (a) Aligned F8BT fibers from THF/DMSO. (b) Fiber with a bead, from THF. Higher magnification SEM (c–d) and corresponding confocal micrographs (e–f) (with higher magnification in the insets) for fibers as in (a) and (b), respectively. Scale bar = 20 μm (a), 5 μm (b), 1 μm (c, d, e, f), 500 nm (insets in e and f), and 100 nm (insets in c and d).

with 0.1 μm spatial resolution. The Raman signal is dispersed using a 0.64 m monochromator equipped with a single 110 × 110 mm^2 grating with 600 lines/mm and detected with a Si charge-coupled device (CCD) cooled at 140 K.[25,26]

Confocal fluorescence microscopy is carried out by an inverted microscope equipped with a scanning laser confocal head (Olympus FV1000). Fibers are excited by a diode laser emitting at 405 nm through microscope objectives with numerical aperture (NA) of 0.7, 0.85, and 1.4 (oil immersion objective). Polarized fluorescence is imaged by inserting absorption polarizers along the optical path.

Polarized PL is investigated by using the linearly polarized light of the 472 nm line of an Ar$^+$ laser coupled to an inverted microscope (IX-71, Olympus). The light emitted by fibers, collected by the microscope objective, is coupled into an optical fiber and analyzed by a monochromator (iHR320, Yobin Yvon) equipped with a CCD detector (Simphony, Yobin Yvon). A $\lambda/2$ waveplate is inserted along the beam path to allow rotation of the polarization of the incident radiation. Two different polarizers are alternatively inserted before the collecting optical fiber to analyze the emitted light. All the spectra are corrected from the contributions introduced by microscope optics. Each spectrum is first normalized by the exciting laser power and then the spectral responses of the optical system are measured
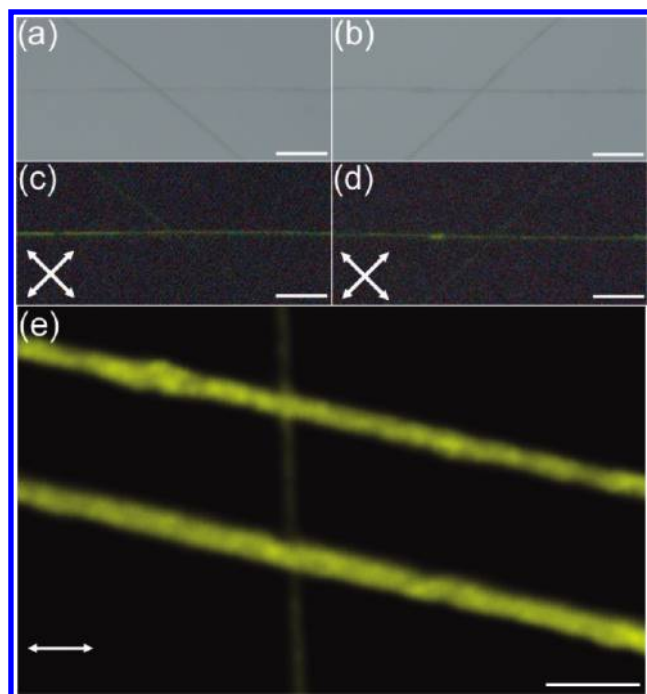
Figure 2. Bright-field optical micrographs of fibers from THF/DMSO (a) and from THF (b) and corresponding POM images (c) and (d), collected with sample between crossed polarizers (whose polarization direction is schematized by the white arrows). (e) Confocal PL micrograph of fibers whose emitted light is analyzed by a polarizer with axis at around 13° with respect to the bright fibers (white arrow). Scale bar = 5 μm.

Figure 3. FTIR spectra of F8BT fiber arrays from (a) THF/DMSO and (b) THF with excitation light polarized parallel (solid line) and perpendicular (dashed line) to fibers. The dashed rectangles evidence the peak regions analyzed for evaluating dichroic ratios.

for light polarized along the two orthogonal directions (X and Y) by using a W lamp as light source and used to correct the corresponding PL spectra.

3. RESULTS AND DISCUSSION

Our fibers are shown in Figure 1. Samples from DMSO/THF show no beads (Figure 1a), which are instead present when using THF with linear density around 10 mm^{-1} (Figure 1b), and they are collectable with a certain degree of mutual alignment (Figure 1b) upon optimizing the applied electric field and interelectrode distance.[8] Fibers from THF/DMSO and THF also have different surface morphology, the former exhibiting complex structures with irregular alternating recessed and protruding sub-100 nm features (Figure 1c). These can origin from both the aggregation and partial precipitation of polymer molecules in the mixture because of their poor solubility in DMSO[27] and Marangoni convective effects due to the higher surface tension and boiling point of DMSO with respect to THF.[28] Fibers from THF present instead a smooth surface with some shallow recessed features (Figure 1d). Similar morphologies are also evidenced by fluorescence confocal microscopy (Figure 1e and 1f).

To investigate the achieved optical anisotropy, first crossed electrospun nanofibers are collected between successive depositions and imaged by POM. We detect maximum brightness for fibers positioned nearly at 45° to crossed polarizers, and extinction for fibers along either parallel or perpendicular orientations with respect to the polarizers (Figure 2). This behavior is typically observed in crystalline materials and in stressed,
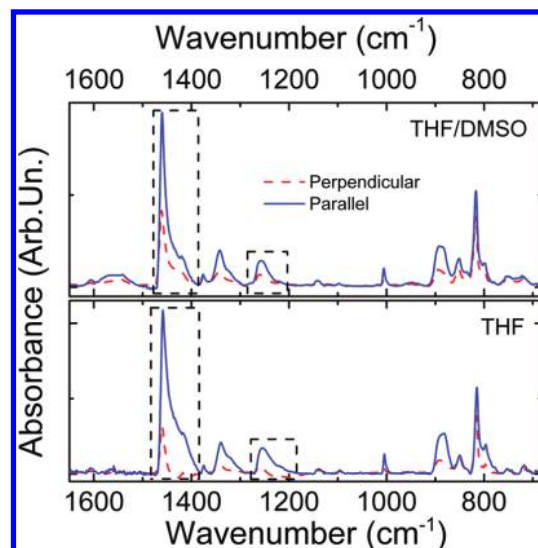
stretched, or flow-aligned glasses and polymers,[29−31] and it is evidence of the uniaxial alignment of the polymer chains along the fiber axis (Z). Polarized PL[20,29,32] confocal microscopy also highlights the fiber optical anisotropy (Figure 2e), showing that the emission intensity from the fiber with axis parallel to that of the polarization analyzer (PL$_{//}$) is nearly four times higher than that with perpendicular axis (PL$_{\perp}$).

FTIR absorption spectroscopy on uniaxially aligned arrays of fibers electrospun from THF/DMSO and THF (Figure 3a and 3b, respectively) is performed by using light polarized parallel and orthogonal with respect to the axis of preferential alignment in the array. Peaks corresponding to the C−H rocking mode (813 cm^{-1}),[33] the C−C stretching mode between phenylene rings (1253 and 1343 cm^{-1}),[34,35] the alkyl chain C−H bending (1377 cm^{-1}),[33] the ring breathing mode (1460 cm^{-1}),[33] and the ring stretching mode of benzothiadiazole (BT) and fluorene (F8) units (1545 and 1605 cm^{-1}, respectively)[34] are observed. Fibers preferentially absorb light polarized parallel to their axes, which is coherent with a favored alignment of the polymer molecules along the fiber axis.[36] For instance, we consider the modes peaked at 1253 and 1460 cm^{-1} and calculate the infrared absorption dichroic ratio, R_{IR}, as the ratio between the absorption peak intensity for light polarized parallel and perpendicular to the array axis. For the modes at 1253 and 1460 cm^{-1}, we obtain a dichroic ratio of 2 and 3 for fibers spun from THF/DMSO and THF, respectively, evidencing a higher degree of molecular orientation in the latter fibers.

To quantitatively evaluate the molecular orientation in single fibers, we employ microscopic polarized Raman spectroscopy, focusing on the 1545 and 1605 cm^{-1} modes. These are typical of F8BT and present a highly uniaxial Raman tensor with principal axis along the chain direction, weakly depending on the details of the chemical structure and therefore especially suitable as a probe of the molecular orientation.[12,37] It is noteworthy to observe that the ES process, even upon adding a nonsolvent such as DMSO, does not introduce significant variations with respect to the corresponding reference films, as appreciable
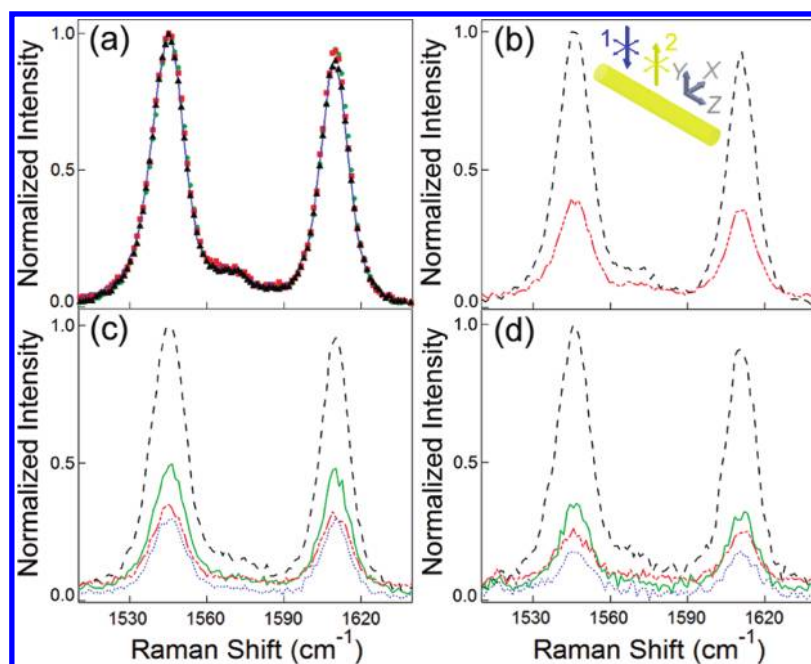
Figure 4. (a) Raman scattering spectra from single fibers from THF (circles) and THF/DMSO (squares) and corresponding reference films (solid line and triangles), respectively. Minor variations in the peak positions[12] from 1545 and 1605 cm^{-1} are common to all the spectra and attributed to intrinsic properties of the employed polymer batch. (b) Spectra from reference F8BT films, measured in the $Z|Z$ (dashed line) and $Z|X$ (dashed-dotted line) configurations. Inset: Experiment geometry. X:, direction perpendicular to the fiber axis in the sample plane; Y, propagation direction of incident laser light (arrow 1) and of backscattered light (arrow 2); Z, fiber axis. (c−d) Spectra from single fibers from THF/DMSO (c) and THF (d) measured in the $Z|Z$ (dashed lines), $Z|X$ (solid lines), $X|Z$ (dashed-dotted lines), and $X|X$ (dotted lines) configurations.

through the spectral features of the two dominant modes, measured without analyzing the polarization of the output light (Figure 4a).

For measurements with polarized light, we use four geometries ($Z|Z$, $X|X$, $Z|X$, $X|Z$ using the notation "incident polarization|analyzed polarization" as in ref 17 and axes shown in the inset of Figure 4b). (Unoriented) F8BT films spin-cast by THF solutions under parallel ($Z|Z$) and crossed ($Z|X$) polarizers configurations present depolarization ratios, $R_{Z|X}/R_{Z|Z}$, where $R_{Z|X}$ and $R_{Z|Z}$ indicate the Raman scattering intensity in the $Z|X$ and $Z|Z$ configurations, respectively, around 0.35 (Figure 4b). Similar values are found for films spin-cast from THF/DMSO. For single electrospun fibers, the strongest and the weakest peaks are found in the $Z|Z$ and $X|X$ configuration, respectively (Figure 4c and 3d). According to the description of the orientation distribution function introduced by Fraser,[38] for the case of uniaxially oriented molecular chains[14] a fraction (f) of molecules are perfectly oriented along the stretching axis (Z) whereas isotropic orientation is assumed for the remaining fraction of molecules ($1 − f$). The oriented fraction can be determined by polarized Raman measurements, if the Raman tensor of the investigated vibrations is known.[14] For our dominant modes, f can be related to the Raman anisotropy, $R_a = R_{Z|Z}/R_{X|X}$, where $R_{X|X}$ is the Raman scattering intensity in the $X|X$ configuration, namely, $f = (R_a − 1)/(R_a + 4)$. From data of Figure 4c−d, we obtain $f_T = 0.6$ and $f_{T−D} = 0.3$ for fibers from THF and THF/DMSO, respectively. These values, uniform along the fiber axis, together with the polarized FTIR absorption data indicate that the THF solvent allows enhanced molecular orientation along the fiber axis. Such findings can be rationalized by taking into account the presence of irregular aggregates in fibers electrospun from THF/DMSO (Figure 1), which are likely formed by tightly

coiled and disordered molecular chains and increase the randomly oriented fraction of molecules.

We also investigate the PL anisotropy, by polarized excitation/detection of the emission from single fibers. Using excitation light polarized along Z, the PL collected with the analyzer parallel to the fiber axis ($I_{Z|Z}$) is more intense than that collected with orthogonal analyzer ($I_{Z|X}$). A similar result holds for excitation polarized along X. We then calculate the PL polarization ratio, $P_i = I_{//,i}/I_{\perp,i}$, and polarization anisotropy, $r_i(E) = [I_{//,i}(E) − I_{\perp,i}(E)]/[I_{//,i}(E) + 2I_{\perp,i}(E)]$,[7,14] where $I_{//,i}$ ($I_{\perp,i}$) is the emission intensity polarized parallel (perpendicular) to the excitation polarization ($i = Z$ and X), at each photon energy (E). P_Z values around 3 and 5, and P_X around 2 and 4, are found for fibers spun from THF/DMSO (Figure 5a) and THF (Figure 5b), respectively, which confirms a higher degree of molecular alignment along the longitudinal axis of fibers spun from the single solvent.

Upon varying the excitation and detection polarizations, we also evaluate the PL spectral changes, normalizing each spectrum to its peak value. Fibers from THF/DMSO show nearly identical spectra under our four excitation/emission configurations (inset of Figure 5a), whereas the PL peak energy of samples from THF exhibit clearly resolvable shifts ($\cong$50 meV, inset of Figure 5b), maximized under configurations with the emission polarized perpendicular to the alignment direction ($Z|X$ and $X|X$). This finding suggests that the excitonic emission from the uniaxially aligned chains is associated with lower transition energies compared to that from randomly aligned molecules and is explained assuming that the alignment in the polymer fibers leads to a reduced interchain separation, on its turn inducing an increased intermolecular electronic delocalization and a red shift of the PL peak emission energy.[7] Such hypothesis is further corroborated by the fact that the PL collected in the $Z|Z$
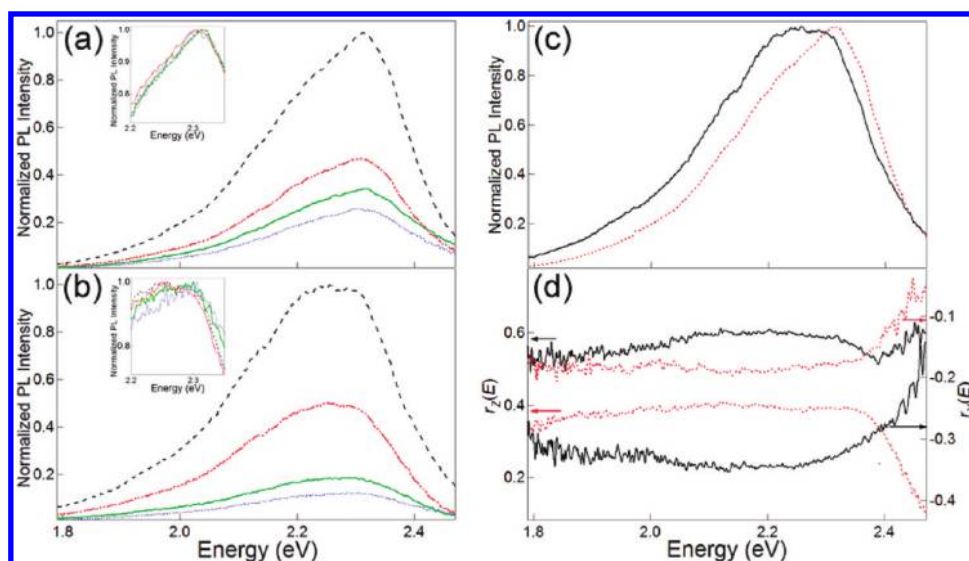
20402

dx.doi.org/10.1021/jp204582j |*J. Phys. Chem. C* 2011, 115, 20399–20405

Figure 5. Polarized PL spectra from single fibers from THF/DMSO (a) and from THF (b) with $Z|Z$ (dashed lines), $Z|X$ (solid lines), $X|Z$ (dashed-dotted lines), and $X|X$ (dotted lines) configurations. The insets in (a) and (b) display the peak regions of the normalized PL spectra. (c) Comparison between PL spectra of a single fiber from THF/DMSO (dashed line) and from THF (solid line) measured in the $Z|Z$ configuration. (d) PL polarization anisotropy spectra for single fibers from THF (solid lines) and THF/DMSO (dashed lines) for excitation polarization parallel (left vertical scale) and orthogonal (right scale) to the fiber longitudinal axis.

configuration from the species more ordered at the molecular level (i.e., single fibers from THF) is red-shifted (60 meV) with respect to that from less ordered species, spun from THF/DMSO (Figure 5c). As a consequence, one also concludes that eventual low-energy sites, as resulting from nanoscale aggregates in fibers from THF/DMSO solutions, are likely nonemissive given the relatively higher emission energy from these samples, a similar effect as that observed in spin-cast F8BT films upon annealing.[34]

Indeed, the observed PL red shift in samples from THF solutions is promptly rationalized by taking into account the eventually different chain packing in the two classes of fibers. For instance, in spin-cast films it is suggested that the polymer packing geometry of high molecular weight F8BT typically presents BT units in neighboring chains adjacent to one another.[34] This supramolecular arrangement, promoted by a relatively fast processing to obtain solid-state samples, does not allow the system to reach a lower energy configuration. On the contrary, low molecular weight F8BT species or, generally speaking, chains of the conjugated polymer which are able to arrange in a more energetically favorable structure, can reach a configuration with alternating BT and F8 units between adjacent molecular chains. These may in turn be associated with reduced interchain energy transfer, and with a concomitant increase in the molecule planarity as observable by complementary Raman measurements.[34]

We believe that similar considerations apply to the fast electrospinning process. Fibers spun from THF are supposed to present a more random configuration of BT-F8 units between adjacent molecular chains with respect to fibers spun from THF/DMSO, due to the higher boiling point of DMSO that allows the polymer chains to arrange in a more energetically favorable structure. This is consistent with the presence of closer BT units in neighboring chains, resulting in more efficient energy transfer from high to low energy states[34] and therefore in a red-shifted PL emission with respect to that of THF/DMSO fibers. However,

from our Raman measurements, we cannot appreciate significant differences in the molecular conformation and degree of planarity between our two classes of fibers as observable by comparing the relative signal intensities in the region 1340−1360 cm^{-1} (C−H and C−C stretches, within and across the BT and F8 units).[34]

The energy dependence of the emission anisotropy for excitation polarized parallel and orthogonal to the fiber axis is displayed in Figure 5d. For reference films, $r(E)$ is generally low (<0.1) and almost constant, whereas for fibers from THF its absolute value is up to 0.6 and larger than for fibers from the mixture at all the photon energies, confirming the higher molecular alignment. For fibers from THF/DMSO, r_Z increases upon decreasing energy down to 2.3 eV and shows a weak spectral dependence for lower energies, as already reported for as-spun F8BT fibers.[39] The slight reduction of the optical anisotropy below 2.3 eV is in agreement with the occurrence of excitonic hopping processes within the fiber.[7,39] For fibers from THF, r_Z shows instead a derivative-like shape around 2.3 eV, related to the PL peak shift measured for $Z|Z$ and $Z|X$ configurations (inset of Figure 5b),[7] and to the increased intermolecular electronic delocalization. Finally, for excitation polarized perpendicularly to the fiber longitudinal axis, the emission anisotropy is negative (Figure 5b), meaning that the PL component with polarization parallel to the fiber longitudinal axis is always larger than that with orthogonal polarization, thus further indicating the achieved molecular order.

4. CONCLUSION

In conclusion, we electrospin conjugated polymer fibers from a single solvent (THF) and a mixture of solvents (THF/DMSO), performing polarized infrared, Raman, and PL spectroscopies to evidence the resulting molecular orientation. A fraction of ordered molecules of 0.6 and a PL polarization ratio up to 5 are found along the axis of fibers from THF, making these

20403

dx.doi.org/10.1021/jp204582j |*J. Phys. Chem. C* 2011, 115, 20399–20405

materials and systems exploitable as anisotropic light nano-sources in optoelectronics and lab-on-chips.

■ AUTHOR INFORMATION

Corresponding Author
*E-mail: andrea.camposeo@cnr.it (A.C.); dario.pisignano@uni-salento.it (D.P.).

Present Addresses
∥Cavendish Laboratory, University of Cambridge, J. J. Thomson Avenue, Cambridge CB3 0HE, U.K.
¶CNR—Istituto di Fisica Applicata "Nello Carrara", via Madonna del Piano 1, I-50019, Sesto Fiorentino, Florence, Italy and NEST, Istituto Nanoscienze CNR and Scuola Normale Superiore , Piazza San Silvestro 12, I-56127 Pisa, Italy.

■ REFERENCES

(1) Barford, W. *Electronic and optical properties of conjugated polymers*; Clarendon Press: Oxford, U.K., 2005.

(2) Redecker, M.; Bradley, D. D. C.; Inbasekaran, E. P.; Woo, E. P. Mobility enhancement through homogeneous nematic alignment of a liquid-crystalline polyfluorene. *Appl. Phys. Lett.* **1999**, *74*, 1400.

(3) Sirringhaus, H.; Wilson, R. J.; Friend, R. H.; Inbasekaran, M.; Woo, E. P.; Grell, M.; Bradley, D. D. C. Mobility enhancement in conjugated polymer field-effect transistors through chain alignment in a liquid-crystalline phase. *Appl. Phys. Lett.* **2000**, *77*, 406.

(4) Long, X.; Grell, M.; Malinowski, A.; Bradley, D. D. C.; Inbasekaran, M.; Woo, E. P. Spectral narrowing phenomena in the emission from a conjugated polymer. *Opt. Mater.* **1998**, *9*, 70.

(5) Virgili, T.; Lidzey, D. G.; Grell, M.; Walker, S.; Asimakis, A.; Bradley, D. D. C. Completely polarized photoluminescence emission from a microcavity containing an aligned conjugated polymer. *Chem. Phys. Lett.* **2001**, *341*, 219.

(6) Virgili, T.; Lidzey, D. G.; Grell, M.; Bradley, D. D. C.; Stagira, S.; Zavelani-Rossi, M.; De Silvestri, S. Influence of the orientation of liquid crystalline poly(9,9-dioctylfluorene) on its lasing properties in a planar microcavity. *Appl. Phys. Lett.* **2002**, *80*, 4088.

(7) Schmid, S. A.; Yim, K. H.; Chang, M. H.; Zheng, Z.; Huck, W. T. S.; Friend, R. H.; Kim, J. S.; Herz, L. M. Polarization anisotropy dynamics for thin films of a conjugated polymer aligned by nano imprinting. *Phys. Rev. B* **2008**, *77*, 115338.

(8) Pagliara, S.; Camposeo, A.; Polini, A.; Cingolani, R.; Pisignano, D. Electrospun light-emitting nanofibers as excitation source in micro-fluidic devices. *Lab Chip* **2009**, *9*, 2851.

(9) Hagler, T. W.; Pakbaz, K.; Voss, K. F.; Heeger, A. J. Enhanced order and electronic delocalization in conjugated polymers oriented by gel processing in polyethylene. *Phys. Rev. B* **1991**, *44*, 8652.

(10) Dyreklev, P.; Berggren, M.; Inganäs, O.; Andersson, M. R.; Wennerström, O.; Hjertberg, T. Polarized electroluminescence from an oriented substituted polythiophene in a light emitting diode. *Adv. Mater.* **1995**, *7*, 43.

(11) Bolognesi, A.; Botta, C.; Martinelli, M.; Porzio, W. Polarized photoluminescence and electroluminescence in oriented films of regioregular poly(3-alkylthiophenes). *Org. Electron.* **2000**, *1*, 27.

(12) Liem, H.-M.; Etchegoin, P.; Whitehead, K. S.; Bradley, D. D. C. Raman anisotropy measurements: An effective probe of molecular orientation in conjugated polymer thin films. *Adv. Func. Mater.* **2003**, *13*, 66.

(13) Cimrová, V.; Remmers, M.; Neher, D.; Wegner, G. Polarized light emission from LEDs prepared by the Langmuir—Blodgett technique. *Adv. Mater.* **1996**, *8*, 146.

(14) Zheng, Z.; Yim, K.-H.; Saifullah, S. M.; Welland, M. E.; Friend, R. H.; Kim, J.-S.; Huck, T. S. Uniaxial alignment of liquid-crystalline conjugated polymers by nanoconfinement. *Nano Lett.* **2007**, *7*, 987.

(15) Di Benedetto, F.; Camposeo, A.; Pagliara, S.; Mele, E.; Persano, L.; Stabile, R.; Cingolani, R.; Pisignano, D. Patterning of light-emitting conjugated polymer nanofibres. *Nat. Nanotechnol.* **2008**, *3*, 614.

(16) Liu, H.; Reccius, C. H.; Craighead, H. G. Single electrospun regioregular poly(3-hexylthiophene) nanofiber field-effect transistor. *Appl. Phys. Lett.* **2005**, *87*, 253106.

(17) Bellan, L. M.; Craighead, H. G. Molecular orientation in individual electrospun nanofibers measured via polarized Raman spectroscopy. *Polymer* **2008**, *49*, 3125.

(18) Reneker, D. H.; Yarin, A. L.; Fong, H.; Koombhongse, S. J. Bending instability of electrically charged liquid jets of polymer solutions in electrospinning. *J. Appl. Phys.* **2000**, *87*, 4531.

(19) Han, T.; Reneker, D. H.; Yarin, A. L. Buckling of jets in electrospinning. *Polymer* **2007**, *48*, 6064.

(20) Pagliara, S.; Camposeo, A.; Cingolani, R.; Pisignano, D. Hierarchical assembly of light-emitting polymer nanofibers in helical morphologies. *Appl. Phys. Lett.* **2009**, *95*, 263301.

(21) Liu, Y.; Antaya, H.; Pellerin, C. Structure and phase behavior of the poly(ethylene oxide)—thiourea complex prepared by electrospinning. *J. Phys. Chem. B* **2010**, *114*, 2373.

(22) Liang, W.; Martin, C. R. Template-synthesized polyacetylene fibrils show enhanced supermolecular order. *J. Am. Chem. Soc.* **1990**, *112*, 9666.

(23) Cai, Z.; Lei, J.; Liang, W.; Menon, V.; Martin, C. R. Molecular and supermolecular origins of enhanced electronic conductivity in template-synthesized polyheterocyclic fibrils. 1. Supermolecular effects. *Chem. Mater.* **1991**, *3*, 960.

(24) Gather, M. C.; Bradley, D. D. C. An improved optical method for determining the order parameter in thin oriented molecular films and demonstration of a highly axial dipole moment for the lowest energy π—π* optical transition in poly(9,9-dioctylfluorene-*co*-bithiophene). *Adv Funct. Mater.* **2007**, *17*, 479.

(25) Scamarcio, G.; Vitiello, M. S.; Spagnolo, V.; Kumar, S.; Williams, B. S.; Hu, Q. Nanoscale heat transfer in quantum cascade lasers. *Physica E* **2008**, *40*, 1780.

(26) Vitiello, M. S.; Scamarcio, G.; Spagnolo, V. Temperature dependence of thermal conductivity and boundary resistance in THz quantum cascade lasers. *IEEE J. Select. Top. Quantum Electron.* **2008**, *14*, 431.

(27) Wannatong, L.; Sirivat, A.; Supaphol, P. Effects of solvents on electrospun polymeric fibers: Preliminary study on polystyrene. *Polym. Int.* **2004**, *53*, 1851.

(28) Luo, S.-C.; Douglas, E. P. Ruptured conjugated polymer thin films formed during spin coating. *J. Polym. Sci. Polym. Phys.* **2006**, *44*, 79.

(29) O'Carroll, D.; Redmond, G. Highly anisotropic luminescence from poly(9,9-dioctylfluorene) nanowires doped with orientationally ordered β-phase polymer chains. *Chem. Mater.* **2008**, *20*, 6501.

(30) Hensley, D. A. *The light microscopy of synthetic polymers*; Oxford University Press: New York, 1984.

(31) Robinson, P. C.; Bradbury, S. *Qualitative polarized light microscopy*; Oxford University Press: New York, 1992.

(32) Wu, J.; Gross, A. F.; Tolbert, S. H. Host—guest chemistry using an oriented mesoporous host: Alignment and isolation of a semiconducting polymer in the nanopores of an ordered silica matrix. *J. Phys. Chem. B* **1999**, *103*, 2374.

(33) Zhao, W.; Cao, T.; White, J. M. On the origin of green emission in polyfluorene polymers: The roles of thermal oxidation degradation and cross-linking. *Adv. Funct. Mater.* **2004**, *14*, 783.

(34) Donley, C. L.; Zaumseil, J.; Andreasen, J. W.; Nielsen, M. M.; Sirringhaus, H.; Friend, R. H.; Kim, J. S. Effects of packing structure on the optoelectronic and charge transport properties in poly(9,9-di-*n*-octylfluorene-*alt*-benzothiadiazole). *J. Am. Chem. Soc.* **2005**, *127*, 12890.

(35) Ariu, M.; Lidzey, D. G.; Bradley, D. D. C. Influence of film morphology on the vibrational spectra of dioctyl substituted polyfluorene (PFO). *Synth. Met.* **2000**, *111−112*, 607.

(36) Tu, D.; Pagliara, S.; Camposeo, A.; Persano, L.; Cingolani, R.; Pisignano, D. Single light-emitting polymer nanofiber field-effect transistors. *Nanoscale* **2010**, *2*, 2217.

(37) Liem, H.-M.; Etchegoin, P.; Bradley, D. D. C. Anomalous Raman scattering from the surface of conjugated polymer melts. *Phys. Rev. B* **2001**, *64*, 144209.

(38) Fraser, R. D. B. The interpretation of infrared dichroism in fibrous protein structures. *J. Chem. Phys.* **1953**, *21*, 1511.

(39) Pagliara, S.; Camposeo, A.; Mele, E.; Persano, L.; Cingolani, R.; Pisignano, D. Enhancement of light polarization from electrospun polymer fibers by room-temperature nanoimprint lithography. *Nanotechnology* **2010**, *21*, 215304.

20405

dx.doi.org/10.1021/jp204582j |*J. Phys. Chem. C* 2011, 115, 20399–20405